The FEBS Journal

FEBS PRESS science publishing by scientists

EDITOR'S CHOICE

The GRASP domain in golgi reassembly and stacking proteins: differences and similarities between lower and higher Eukaryotes

Luís F. S. Mendes[1], Natália A. Fontana[1], Carolina G. Oliveira[1], Marjorie C. L. C Freire[2], José L. S. Lopes[3], Fernando A. Melo[4] and Antonio J. Costa-Filho[1]

1 Departamento de Física, Faculdade de Filosofia Ciências e Letras de Ribeirão Preto, Universidade de São Paulo, Ribeirão Preto, Brazil
2 Centro de Pesquisas Aggeu Magalhães – Fundação Oswaldo Cruz (FIOCRUZ- PE), Recife, Brazil
3 Departamento de Física Aplicada, Instituto de Física, Universidade de São Paulo, São Paulo, Brazil
4 Departamento de Física, Centro Multiusuário de Inovação Biomolecular, IBILCE, Universidade Estadual Paulista Júlio Mesquita, São Paulo, Brazil

Keywords
eukarya; golgi reassembly and stacking protein; GRASP domain; intrinsically disordered regions; spectroscopy

Correspondence
A. J. Costa-Filho, DF/FFCLRP/USP, Av. Bandeirantes 3900, Ribeirão Preto, SP 14040-901, Brazil
Tel: +551633153665
E-mail: ajcosta@usp.br

(Received 18 January 2019, revised 18 March 2019, accepted 29 April 2019)

doi:10.1111/febs.14869

The Golgi complex is part of the endomembrane system and is responsible for receiving transport cargos from the endoplasmic reticulum and for sorting and targeting them to their final destination. To perform its function in higher eukaryotic cells, the Golgi needs to be correctly assembled as a flattened membrane sandwich kept together by a protein matrix. The precise mechanism controlling the Golgi cisternae assembly is not yet known, but it is widely accepted that the Golgi Reassembly and Stacking Protein (GRASP) is a main component of the Golgi protein matrix. Unlike mammalian cells, which have two GRASP genes, lower eukaryotes present only one gene and distinct Golgi cisternae assembly. In this study, we performed a set of biophysical studies to get insights on the structural properties of the GRASP domains (DGRASPs) from both human GRASP55 and GRASP65 and compare them with GRASP domains from lower eukaryotes (*Saccharomyces cerevisiae* and *Cryptococcus neoformans*). Our data suggest that both human DGRASPs are essentially different from each other and that DGRASP65 is more similar to the subgroup of DGRASPs from lower eukaryotes in terms of its biophysical properties. GRASP55 is present mainly in the Golgi medial and *trans* faces, which are absent in both fungi, while GRASP65 is located in the *cis*-Golgi. We suggest that the GRASP65 gene is more ancient and that its paralogue GRASP55 might have appeared later in evolution, together with the medial and *trans* Golgi faces in mammalians.

Introduction

The Golgi complex is part of the endomembrane system and is responsible for receiving transport cargos from the endoplasmic reticulum to sort and to target them to their final destination [1,2]. Furthermore, this organelle works as the main glycosylation hub inside the cell and is also responsible for many lipid syntheses

Abbreviations
ANS, 1-anilino-8-naphthalenesulfonic acid; CD, circular dichroism; CnDGRASP, *Cryptococcus neoformans* GRASP GRASP domain; CUPS, compartments of unconventional protein secretion; DGRASP55, human GRASP55 GRASP domain; DGRASP65, human GRASP65 GRASP domain; GRASP, Golgi reassembly and stacking protein; IDP, intrinsically disordered protein; IDR, intrinsically disordered regions; NMR, nuclear magnetic resonance; ScDGRASP, *Saccharomyces cerevisiae* GRASP GRASP domain; SPR, Serine- and Proline-rich domain; SRCD, synchrotron radiation circular dichroism; UPS, unconventional protein secretion.

[1,2]. In order to achieve such an expressive number of functionalities in higher eukaryotic cells, the Golgi needs to be correctly assembled as a flattened membrane sandwich kept together by a protein matrix [1]. The disruption of this assembly ultimately leads to failure in correct protein glycosylation and sorting, besides protein secretion impairment [1,3–5].

It has been largely accepted that the Golgi Reassembly and Stacking Protein (GRASP) are part of the Golgi protein matrix [6–8]. There are two paralogue genes found in mammalians (GRASP55 and GRASP65), which have been suggested to work in synergy to build the Golgi ribbon [8,9]. It has been previously observed that the double knockout of GRASP55 and GRASP65 by CRISPR-Cas9 technology led to a total Golgi fragmentation [10]. Moreover, GRASP silencing also led to incorrect protein glycosylation [3] and accelerated protein transport to the plasma membrane [4]. Both GRASP proteins require a double membrane anchoring to promote their correct transdimerization, responsible for bringing the Golgi cisternae together [11]. While GRASP65 is located mainly in the *cis* part of the Golgi, GRASP55 is present in the medial and *trans* faces [6,7]. These unique localizations of both GRASPs have been explored as Golgi markers for colocalization experiments in several manuscripts [12,13].

Golgi reassembly and stacking proteins are observed in all eukaryotic cells with the exception of plants, where no obvious homologs have been found so far [9,14]. Interestingly, mammalian cells have two GRASP genes [14], while in lower eukaryotic cells, where the correct Golgi cisternae assembly is not a common feature, only one gene has been reported [14]. *Saccharomyces cerevisiae* has one GRASP gene and only 40% of its cisternae are assembled into stacks, whereas in the human pathogen *Cryptococcus neoformans*, which also has one GRASP gene, no Golgi stacks are observed [15,16]. Curiously, *Plasmodium falciparum*, the causative agent of malaria, has in its DNA one GRASP gene that encodes for two GRASP isoforms coming from a splice variant [17]. In this system, the first GRASP relies on a well-conserved myristoylation motif typical of the human GRASPs, while the variant displays a different N terminus, similar to GRASPs found in fungi [17].

Even though GRASPs were initially found as structural factors of the Golgi complex [14], an unusual (and still unclear) participation in unconventional protein secretion (UPS) of several proteins has been observed [18,19]. GRASPs have a fundamental involvement in the stress-induced UPS (more specifically, UPS types 3 and 4 [19]) but their exact role is still a matter of debate [19]. A recent paper has suggested that GRASPs act as a tethering factor of autophagosome accessory proteins needed for the autophagosome–lysosome fusion and also on autophagosome maturation under glucose deprivation [20,21]. Since nutrient starvation is one of the main activators of type 3 UPS, it has been suggested that GRASP might be recruited by the autophagosome and by the plasma membrane to enable the release of the UPS cargo, but this hypothesis is still to be proven. A previous work has suggested a direct (and necessary) interaction of GRASPs with the protein to be secreted, especially in the case of type 4 UPS [22]. This direct interaction with the protein cargo has already been observed in other situations [23–26]. Some specific roles have also emerged, such as the participation in the formation of specific autophagosome-like structures (named compartments of unconventional protein secretion, or CUPS), but regardless of their true nature and existence in yeast [27,28], so far there are no evidences that these structures exist in mammalian cells [29].

The GRASP structure is composed of two main regions, a conserved N-terminal portion with two protozoa-like PDZ domains, called GRASP domain, and a nonconserved C terminus, rich in serine and proline residues and presenting an intrinsically disordered behavior [14,30]. The GRASP domain is the 'functional' region of this protein, acting in the dimerization step during cisternae stacking and also 'grasping' protein partners in an array of different situations [9,14,31]. The C terminus, also known as SPR domain, has a regulatory functionality by means of its phosphorylation [14], cleavage sites [32] and O-GlcNAcylation in nutrient-rich conditions [21]. In terms of its biophysics/biochemistry, the SPR domain is not conserved even inside the same species (GRASP55 and GRASP65, for instance) [14]. It is formed by an unusual combination of aminoacids with several serines and prolines, two of the most disorder-promoting aminoacids [33]. We have shown that, even though the SPRs are not conserved among species in terms of aminoacid sequence, the family shares a highly conserved disorder profile [30]. Such a disorder profile is probably due to the low hydrophobic amino acid content, which compromises the formation of hydrophobic clusters during the protein folding [34]. This means that the SPR domains from different organisms might be very similar in structural terms despite their variations in primary sequence and in total length.

When it comes to the full-length structure, it has been previously reported that the GRASP from *Cryptococcus neoformans* behaves as a native molten globule-like protein, with an overall structural dynamic in μs-ms timescale and high structural plasticity [30]. The

physicochemical perturbations in the surroundings of the biological membrane seem to be the main inducer of disorder-to-order transitions in GRASP [35].

Despite the great number of studies focusing on GRASPs in both the biological and biophysical context, several aspects remain elusive. For instance, although GRASPs are conserved among the GRASP-containing organisms, there are no obvious reasons of why there are two GRASPs in mammalians and only one in lower eukaryotes, and whether GRASP55 and GRASP65 show the same behavior in solution although having distinct functionalities and protein partners [9,14]. Whether the variations seen in the number and behavior of GRASP homologs correlates with the significant variability in the Golgi structure or with the particularities in UPS among different organisms still deserves more attention. In this study, we performed a set of biophysical studies on the GRASP domains of both human GRASP55 and GRASP65 (named DGRASP55 and DGRASP65, respectively) and compare them with two members of GRASPs from lower eukaryotes (*S. cerevisiae* and *C. neoformans*) to get insights on the structural behavior of GRASPs from different system complexities.

Results and Discussions

Secondary structure comparison

The GRASP domain is composed of two PDZ domains connected in tandem [36,37]. PDZs work as protein interaction domains that bind, in a sequence-specific manner, to C-terminal peptides or internal disordered regions [38]. This domain has a very particular secondary structure organization formed by a $\beta\beta_2\beta\alpha\beta\varpi\beta\alpha_2\beta_6$ arrangement, which collapses in a modular structure and where the binding groove is formed by both β_2 and α_2 [36,38]. However, the first GRASP domain structure determined for a member of the GRASP family (DGRASP55) showed that, unlike other eukaryotic PDZ domains, each binding groove was formed by the final (β_6) rather than the second β-strand within the fold [36]. This is a very unusual structural organization for a PDZ domain in eukaryotes but a common fold in prokaryotes [36]. Therefore, GRASPs are formed by uniquely arranged PDZ domains in eukaryotes, which could explain some of the unusual biophysical features previously observed [30,35,39].

The first comparison within the set of GRASP domains under investigation was based on their secondary structure organization, aiming to check for differences and/or conservation. The 3D structures of human DGRASP55 (PDB ID 3RLE), a peptide-bound human DGRASP65 and also the homolog in rat of apo DGRASP65 (PDB IDs 4KFV and 4REY, respectively) have been previously reported [36,37]. Here, we constructed a model of ScDGRASP and CnDGRASP using Swiss-MODEL and then aligned the four GRASP domain structures using Pymol (Fig. 1A). The structures aligned very well, suggesting that they all share the same two-circular permutation PDZ fold, although the amino acid sequence only shares around 30% identity across species (Fig. 1B). The CD spectra show that they all might share a similar secondary structure content, except for CnDGRASP, which presents the most pronounced spectral differences, especially in the region bellow 210 nm (Fig. 1C). Because of the higher magnitude of the minimum and its shift to lower wavelengths (from 208 to 205 nm), we can speculate that this might be a contribution of a more significant number of disordered regions in CnDGRASP secondary structure (Fig. 1C). We reconstructed the CD spectra of both human DGRASPs based on their PDB files by using PDB2CD and the reference database for soluble proteins SP175 (Fig. 2) [40]. The reconstructed CD spectrum of DGRASP55 agrees very well with the experimental one, suggesting that the overall structure is not affected by the crystallographic conditions and packing (Fig. 2A). The same is not observed for the DGRASP65, where the reconstructed CD spectra are very different from the experimental one (Fig. 2B), suggesting that the structure in solution might differ in some degree from the crystallographic ones, even considering the inherent limitations of this reconstruction technique. These data suggest that all GRASP domains conserve the overall pattern of DGRASP55 crystal structure with CnDGRASP having more disordered regions.

The SRCD spectra deconvolution using Dichroweb confirmed our analyses by showing that the GRASP domains share about the same total secondary structure content (Table 1). The similarity observed in the CD spectra allows us to conclude that all GRASP domains used in this work share approximately the same secondary structure organization, although CnDGRASP seem to contain a greater contribution of disordered regions.

Looking for disordered regions within the domains

The SRCD deconvolution data indicated that all GRASP domains have considerable amounts of disordered regions (~40%). We previously reported the existence of intrinsically disordered regions (IDRs) in the

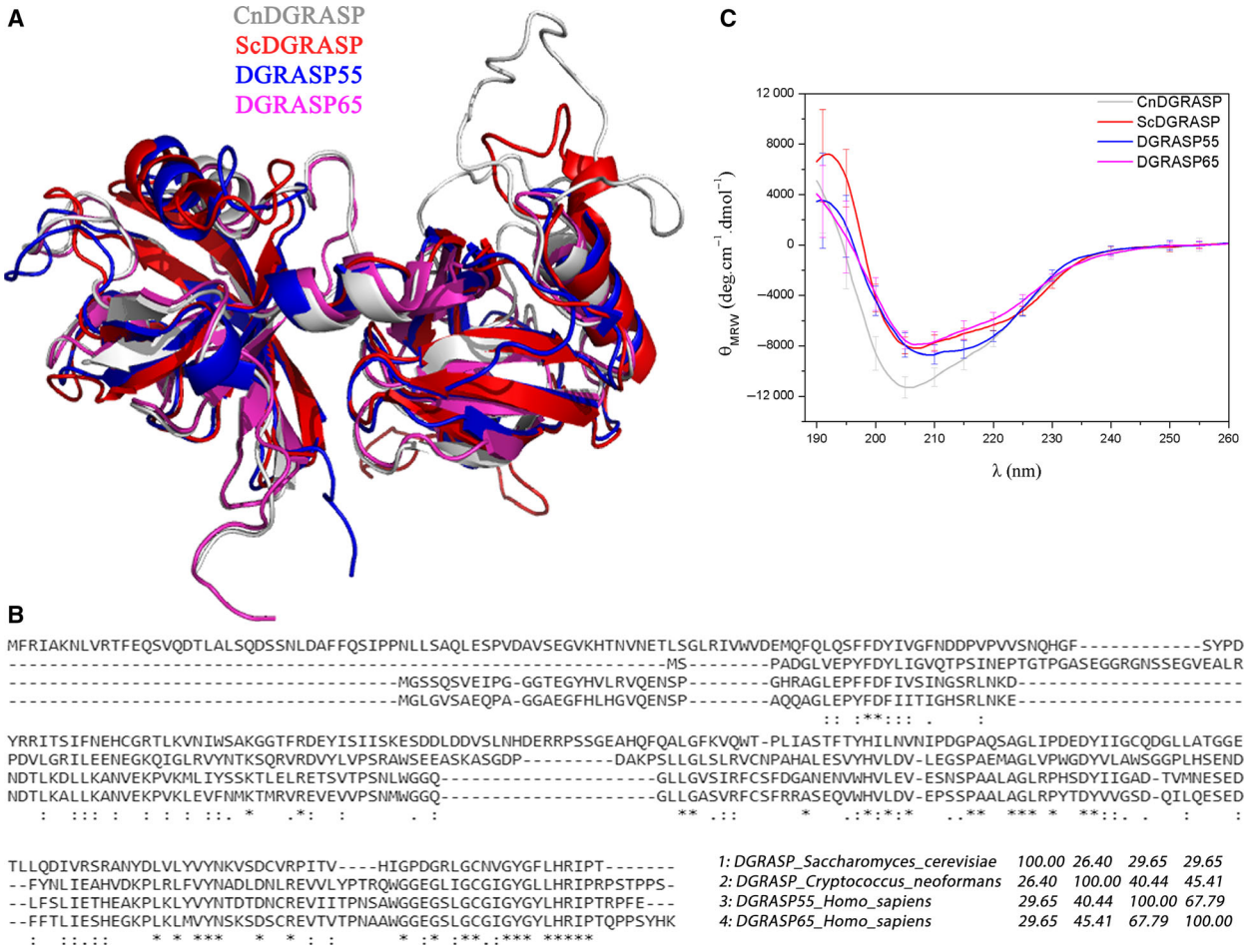

Fig. 1. Structural analyses of different DGRASPs. (A) Molecular modeling structures of CnDGRASP and ScDGRASP constructed using Swiss-Model, superimposed with the crystal structures of human DGRASP55 (PDB ID 3RLE) and rat DGRASP65 (PDB ID 4KFV). (B) Sequence alignment of human DGRASPs, CnDGRASP and ScDGRASP using Clustal Omega. The Percent Identity Matrix is shown in the bottom right, where the numbers vary from 0 to 100 with 100 being the complete alignment of the sequences. (C) Far-UV Circular dichroism spectra of the different GRASP domains. Error bars represent standard deviations of duplicate measurements.

full-length CnGRASP and ScGRASP, especially in the SPR domain [30]. Those conclusions were based on intrinsically disordered predictions and indirect experimental evidences, which impaired more definitive conclusions regarding IDRs in the GRASP domain only. IDRs are inherently sensitive to proteolysis and a proteolytic assay can be used to check for their indirect presence within the GRASP domains [41]. Here, trypsin was used in the limited proteolysis in a direct comparison with the stable and compact protein ovalbumin. As expected, ovalbumin shows an incredible resistance to trypsin activity, a feature already observed previously (Fig. 3) [30]. The fungi DGRASPs are very sensitive to this proteolysis assay (Fig. 3) and it is possible to check that CnDGRASP is totally cleaved within 30 min of incubation, while ScDGRASP was promptly cleaved into two fragments that show some resistance to trypsin, (Fig. 3). DGRASP55 shows the highest resistance to trypsin, with a total stability of at least 24 h, similar to the ovalbumin control (Fig. 3). Interestingly, it can be observed that a small fragment of this protein is cleaved after 30 min but the product is stable over time. We suggest that this might be a small disordered fragment from either the N- or the C terminus, which can be cleaved without compromising the protein core. DGRASP65 still shows some resistance (compared to the fungi DGRASPs) but in a much lesser extent when compared with its paralogue (Fig. 3). The protein core remains stable up to 3 h only, indicating higher IDR content (Fig. 3). The results suggest that both CnDGRASP and ScDGRASP present higher IDR contents than human DGRASPs and that DGRASP65

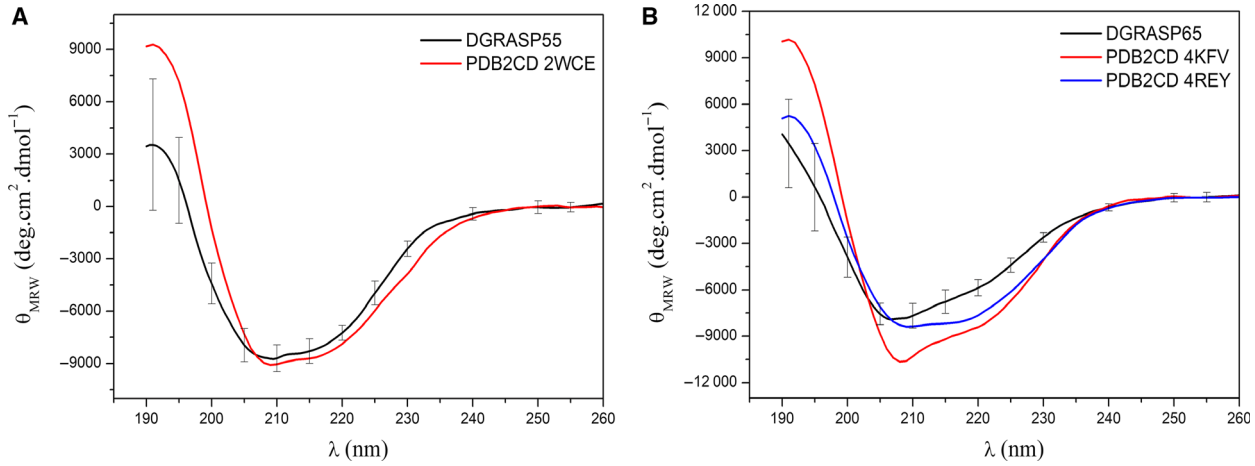

Fig. 2. Circular Dichroism spectra reconstruction based on the PDB structure files were performed using PDB2CD. (A) DGRASP55 experimental CD spectrum (black) with the theoretical CD based on the PDB file 2WCE (red). (B) The same plot for DGRASP65 (black) but using the PDB files 4KFV (Rattus norvegicus homolog—red) and 4REY (crystal structure of the GRASP65-GM130 C-terminal peptide complex—blue). The GM130 C-terminal peptide was removed from the PDB file prior the CD spectrum reconstruction. Error bars represent standard deviations of duplicate measurements.

Table 1. Circular dichroism spectra deconvolution using Dichroweb.

	α-helix	β-sheet	Loop	Disordered	Total	NRMSD
CnDGRASP						
CDSSTR	0.170	0.290	0.140	0.400	1.000	0.007
Selcom3	0.167	0.296	0.133	0.407	1.004	0.339
Contin-LL	0.182	0.287	0.130	0.408	1	0.036
Average	17%	29%	13%	41%		
ScDGRASP						
CDSSTR	0.170	0.330	0.130	0.390	1.000	0.028
Selcom3	0.169	0.297	0.121	0.353	0.940	0.259
Contin-LL	0.182	0.312	0.128	0.378	1.000	0.129
Average	17%	31%	13%	37%		
DGRASP55						
CDSSTR	0.160	0.310	0.130	0.390	0.99	0.023
Selcom3	0.158	0.327	0.127	0.374	0.986	0.203
Contin-LL	0.164	0.324	0.127	0.385	1	0.158
Average	16%	32%	13%	38%		
DGRASP65						
CDSSTR	0.100	0.340	0.130	0.430	1.000	0.020
Selcom3	0.138	0.309	0.133	0.389	0.969	0.130
Contin-LL	0.175	0.287	0.130	0.408	1	0.036
Average	14%	31%	13%	41%		

seems to be somewhat similar to this subgroup than the well-behaved DGRASP55.

Another strategy to indirectly probe whether a protein presents an IDP-like behavior is by checking the effects of dehydration on its secondary structure, which can be monitored by CD or SRCD spectroscopies [41,42]. Unlike IDPs, globular, well-structured proteins exhibit only minor alterations by CD upon removal of bulk water during film formation [42]. We previously observed that the full-length CnGRASP shows significant structural changes upon dehydration, suggesting that the removal of water molecules can induce multiple disorder-to-order transitions [35]. However, no systematic study on the effects of dehydration over the GRASP domains has been performed. The CD spectra obtained from samples containing the GRASP domains under investigation before and after dehydration are shown in Fig. 3. ScDGRASP and CnDGRASP show dramatic changes in the shape of their CD spectra when the bulk water is removed, where an increase in the $\theta_{220\ nm}/\theta_{208\ nm}$ ratio and a significant shift of the peak at 190 nm to ~195 nm are observed (Fig. 4). Both changes suggest an increase in the total regular/ordered secondary structure content [43]. Although the DGRASP65 shows higher exposure of their disordered regions when compared to DGRASP55, both structures are resistant to the dehydration effects, showing only minor changes after protein film formation (Fig. 4). The data suggest that, even though all the DGRASPs chosen in this study present high disordered content (up to 40%), a difference in the packing/total tertiary interactions might expose (or not) these structures to the solution, leading to different accessibility to proteolytic activity and/or disordered-to-order transitions upon reducing the bulk water molecules content.

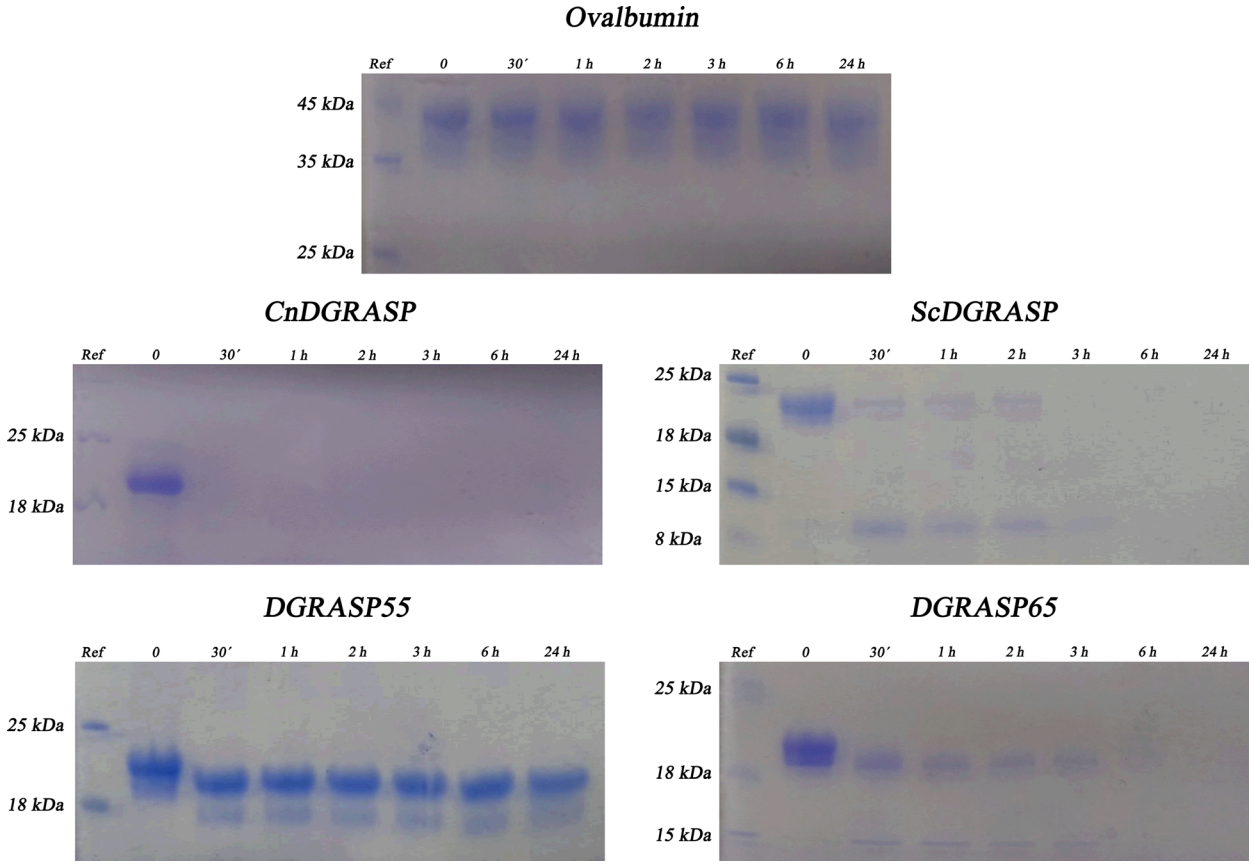

Fig. 3. Proteolysis sensitivity monitored by SDS/PAGE. Different DGRASPs (concentration of 1 mg/mL) incubated with trypsin at a molar ratio of 1 : 100 for time intervals at 25 °C. Ovalbumin, at the same protein:trypsin molar ratio and temperature, was used as a control of well-folded protein. The experiments were performed in triplicate.

DGRASP55 is a better-behaved protein

The simplest thermodynamical and kinetic models for a protein unfolding assume the protein can exist in two conformational states (native and unfolded), separated by a single activation-free energy barrier, and interconverting via a cooperative two-state transition [44]. Therefore, the degree of cooperativity can be used to check how well folded the protein is since this 'well-behaving' is characterized by funnel-like energy landscapes that have a well-defined global energy minimum [33,44]. IDPs and 'not so well-behaved' proteins lack this characteristic global minimum and the unfolding takes place in a less cooperative (or none) way due to multiple intermediate states [33,45]. Thus, one can look for IDP behavior by following the unfolding of a determined protein and checking the cooperativity of the transition, for instance using CD/SRCD experiments.

The chemical unfoldings of the GRASP domains are shown in Fig. 5, where the ellipticities at characteristic wavelengths of the CD spectra are monitored as a function of urea concentration. The data suggest that, even though the fungi DGRASPs possess comparable amounts of ordered secondary structures compared to the human DGRASPs, their transition to the unfolded state takes place in a low cooperative way. ScDGRASP shows some degree of cooperativity but still very far from that observed in DGRASP55. It is possible to observe that DGRASP55 unfolding shows the characteristic sigmoid-like transition, typical of well-behaved proteins [44] with a concentration of half transition centered around 4 M of urea. The data also indicate that DGRASP55 is a stable, well-folded, protein, which agrees with the fact that this protein is capable of forming adequate crystals for X-ray diffraction experiments. However, DGRASP65 does not follow the same pattern (Fig. 5). Although the crystal structure of apo human DGRASP65 is not yet available, there are structures solved for its apo and peptide-bound rat homolog [46,47], suggesting that we could expect a behavior similar to DGRASP55. However, this is not observed in Fig. 5 and the transition to the

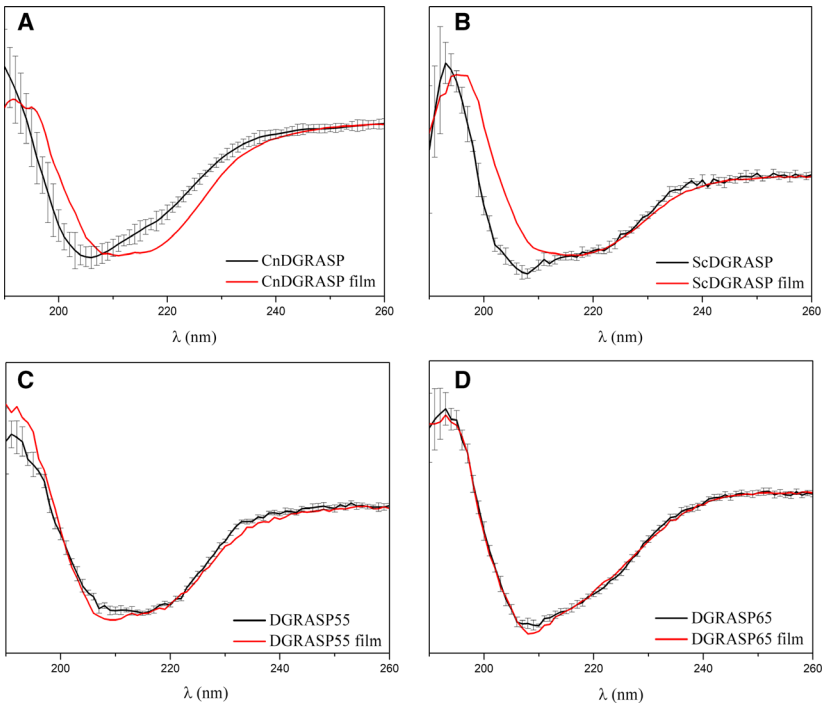

Fig. 4. Secondary structure perturbation after dehydration monitored by SRCD and CD. In each panel, the red line is the spectrum from dried films of the proteins and the black, the control in solution. Error bars represent standard deviations of duplicate measurements.

unfolded state is linear, just like the one observed before for the full-length CnDGRASP [30]. The data indicate that the overall tertiary contacts of DGRASP65 share some of the structural features of the lower eukaryotes DGRASPs, which were previously attributed to be collapsed IDPs/molten globule-like proteins [30,39].

DGRASPs have high IDR content but they are still collapsed proteins

Although rich in IDRs, all the GRASP domains used in this work have collapsed structures and this is easily observed by the maximum of tryptophan fluorescence emission, which are all blue shifted in some degree compared to the emission observed for the tryptophan in solution (Fig. 6A). Furthermore, the hydrophobic core is not easily accessible to the solvent, since the ANS permeation is not significantly high when compared to the unfolded state in 8 M urea (Fig. 5A). Native CnDGRASP is the only one showing high ANS accessibility (Fig. 6B), a phenomenon already observed for the corresponding full-length construction [30]. As it has been previously shown, CnGRASP has a characteristic dynamic conformation in a μs-ms timescale leading to a hydrophobic interior with high water accessibility [30], and we show here that this behavior is also SPR independent. The reason why only CnDGRASP shows this feature is not known but the higher IDR content could expose more hydrophobic regions, which might explain this behavior.

Cryptococcus neoformans GRASP GRASP domain is the only DGRASP tested that has water-exposed hydrophobic sites, which do not include the regions where the Trp residues are located (Fig. 6C). The tryptophan accessibility experiment data using the collisional quencher acrylamide agrees with the ANS experiment and show that all DGRASPs have a collapsed structure (different accessibility compared to the free tryptophan in solution). Trp residues present the same accessibilities to acrylamide between the two fungi DGRASPs and between the two human DGRASPs. The latter ones also show a more collapsed and less accessible protein interior than the fungi ones (Fig. 6C).

High-resolution data confirm that DGRASP65 and 55 are essentially different from each other

Although protein crystallography is not a suitable technique to tackle IDP structural determination, flexibility trends can still be inferred from the temperature factor (B-factor) of the crystal structures [41]. The B-factors of both DGRASP55 and DGRASP65 (PDB ID 3RLE and 4REY with the peptide bounded omitted) are depicted on the respective structures in Fig. 7A. The values observed for DGRASP55 are in the range of 20–30 $Å^2$, suggesting that this protein has a better-defined structure. Those B-factor values are

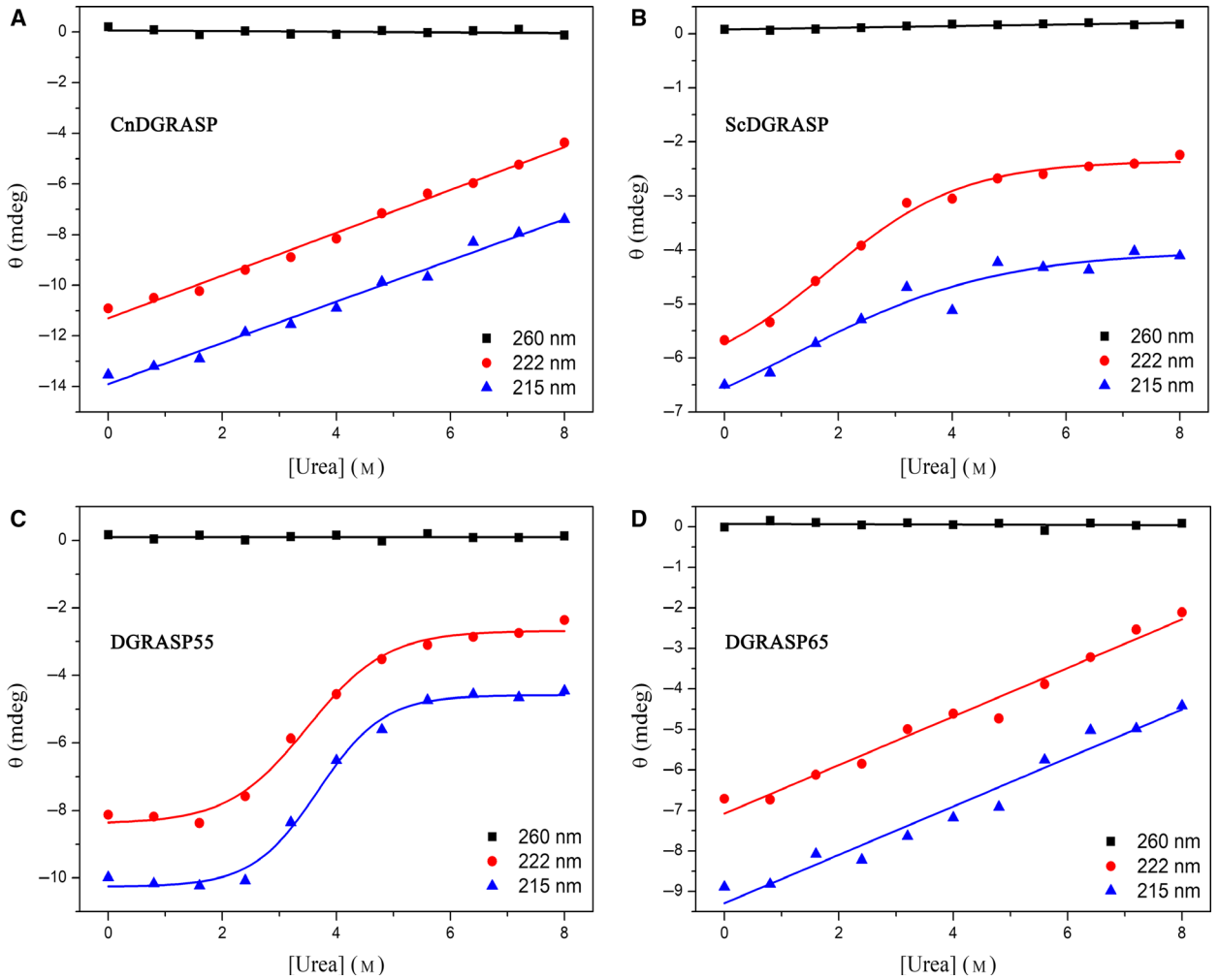

Fig. 5. The DGRASP chemical denaturation using urea as a chaotropic agent. The graphics are showing the variation in ellipticity (mdeg) at different wavelengths (260, 222, 215 nm) during urea titration. A linear function was fitted to the data at 260 nm, representing the stability of the baseline, and to the 220/215 nm of CnDGRASP and DGRASP65. A sigmoidal function was fitted to the 222/215 nm of DGRASP55 and ScDGRASP.

below the up B-factor maximum theoretical limit (around 31 $Å^2$) acceptable for a structure solved at 1.6 Å resolution [48]. DGRASP65 B-factors show a different pattern, with the PDZ2 presenting a smaller B-factor range (similar to DGRASP55), but the PDZ1 being much more flexible, with several regions almost in the limit of total disorder (which is around 60 $Å^2$), and much higher than the B-factor maximum expected for a structure solved at 1.9 Å resolution (around 40 $Å^2$) [48]. Of course, this is not a suggestion that the crystal structures are right or wrong, but rather just an observation that DGRASP65 structure has a tendency of being more flexible than DGRASP55.

Our low-resolution structural characterization presented above indicated that differences between DGRASPs are likely due to differences in IDR content. To further explore this issue, we used NMR to characterize the overall structure of these domains in solution. The ^{1}H-^{15}N HSQC spectrum of DGRASP55 shows that this domain is indeed well folded and has low IDR content, since most of the amide resonances are widely spread from ca. 7 to 10 p.p.m. (Fig. 7B). DGRASP65 is again different with its ^{1}H-^{15}N HSQC spectrum showing several superpositions of amide resonances in the region around 8 p.p.m. and narrower dispersion of the Asn/Gln side chains than that seen for DGRASP55 (Fig. 7B). Nonetheless, DGRASP65 still shows good signal dispersion in its ^{1}H-^{15}N HSQC spectrum, suggesting that, although this protein is enriched in IDRs, it still possesses a good amount of well-ordered structures.

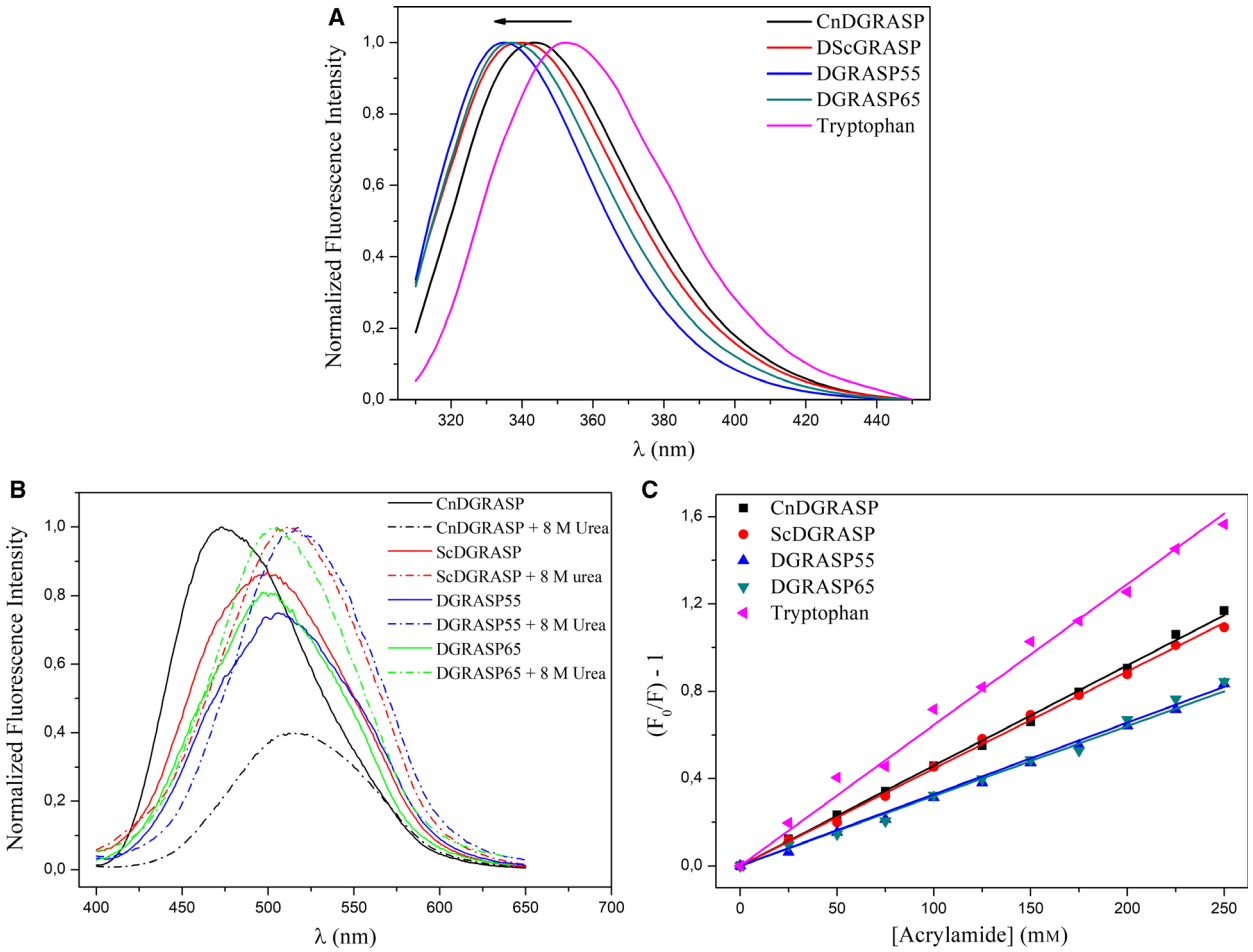

Fig. 6. Protein compaction monitored indirectly using steady-state fluorescence. (A) DGRASPs ANS accessibility. Each pair of spectra (with and without 8 M urea) was normalized dividing both dataset by the highest fluorescence intensity. This procedure indicates that only CnDGRASP has an accessible hydrophobic core in the native state. (B) Fluorescence quenching using acrylamide. The linear Stern–Volmer model was fitted to each dataset and compared to the behavior of free tryptophan in solution.

The ScDGRASP ^{1}H-^{15}N HSQC spectrum is quite similar to the DGRASP65 but the signal crowding around 8 p.p.m. is higher for the former, suggesting that ScDGRASP is formed by an even higher number of IDRs (Fig. 7B). This can be seen clearer in the proton spectrum where the majority of the resonance lines seems to be located (and overlapped) in this very narrow region around 8 p.p.m., especially when compared with the DGRASP65 or DGRASP55 proton spectra (Fig. 7C). Again, CnDGRASP is the most different since the broadening of most of the resonance lines leads them to be out of the sensitivity limit and the few visible peaks in the HSQC NMR spectrum are located around 8 p.p.m. (Fig. 7B). This narrow distribution of resonance lines is more evident when looking to the proton resonance spectra in this range of the amide resonances (Fig. 7C), where both fungi DGRASPs show similar spreading. The amide resonance line broadening follows the same pattern observed previously for the full-length CnGRASP, which was shown to be a molten globule-like protein with a conformational change-dynamic in a μs-ms timescale [35]. These data suggest that the CnDGRASP molten globule-like behavior is SPR independent.

DGRASPs show different behavior upon pH variation

Intrinsically disordered proteins are naturally disordered due to a greater/lower content of charged/hydrophobic residues, respectively [33,49]. It has been shown before that GRASPs do not have a combination of residues typical of fully disordered proteins [30], which agrees with our observations that they do possess ordered structures and are collapsed proteins. However, the presence of IDRs

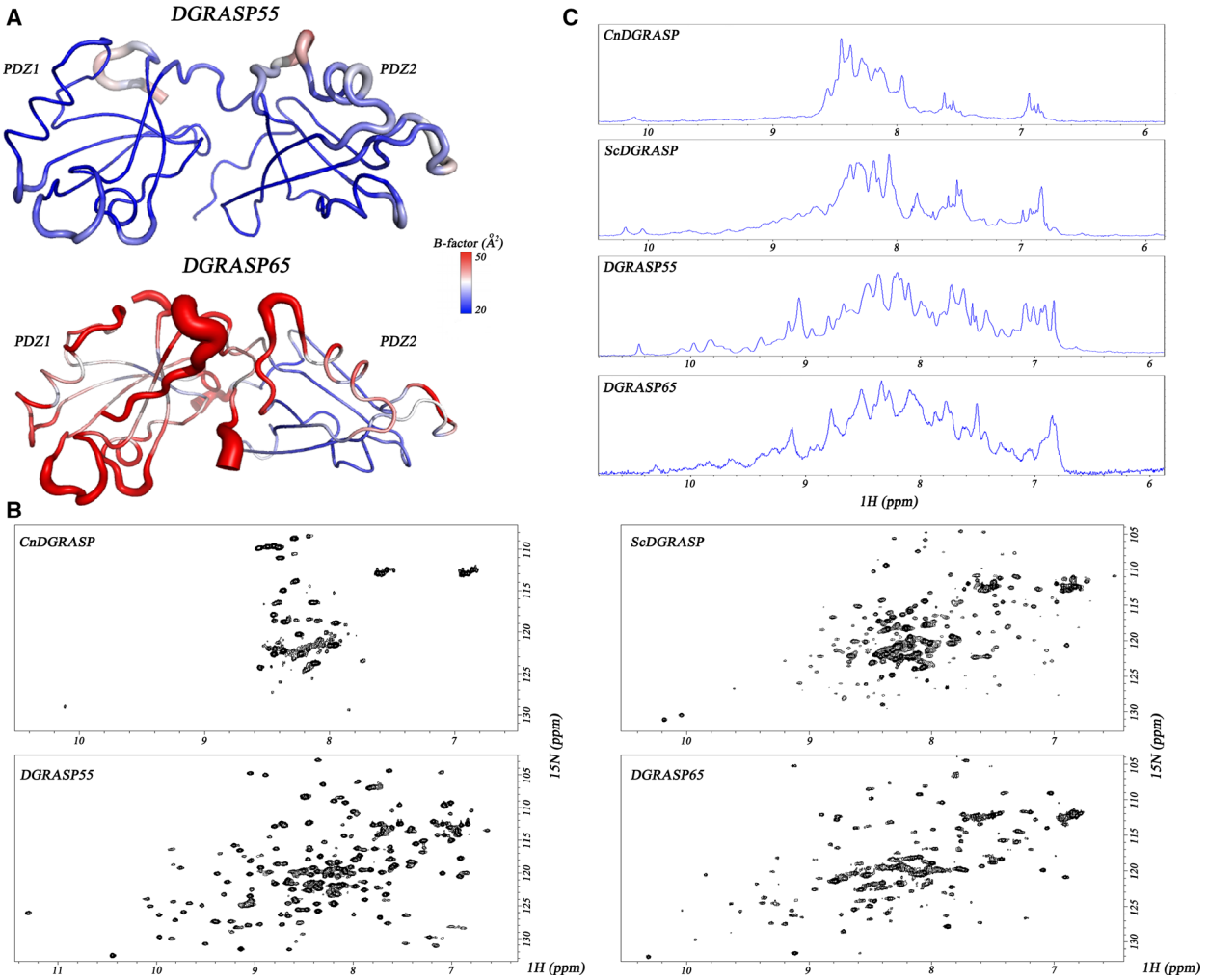

Fig. 7. High-resolution analyses of DGRASP flexibility and disorder. (A) Plot of the crystallographic structure of human DGRASP55 (PDB ID 3RLE) and human DGRASP65 with a peptide bounded which was omitted (PDB ID 4REY), in a color gradient according to their respective B-factor values. (B) 1H-15N HSQC NMR spectra of DGRASPs. (C) DGRASPS 1H NMR spectra of 1H-15N coupled protons.

still leads to some unusual behavior and this might be due to uncompensated charges along those regions. In order to test this hypothesis, we evaluated how the DGRASPs respond to pH-induced charge alterations in their structures by measuring their CD spectra at different pH values (Fig. 8). The secondary structure of CnDGRASP and DGRASP65 seems to be more resistant to pH variation, with only minor changes (within the error bars of the spectra) at higher pHs. CnDGRASP CD at pH 5 seems to be the only one with a change in shape, especially close to 205 nm. This was also previously observed for the full-length CnGRASP and was associated with the fact that this is closer to the theoretical pI of this protein, which is estimated to be 4.9. DGRASP55, however, shows significant changes at low pH (3 and 4). Because the pI of this protein is also around 5, these structural changes are just associated to a regular unfold. ScDGRASP is the one that has the most different and unusual pattern. At pH 3–4, this protein has a huge conformational change in the β-sheet–rich structure, previously observed for the full-length ScGRASP and associated with the formation of a fibril-like supramolecular structure [39]. These data suggest that fibril formation might also take place with the isolated ScDGRASP at lower pHs, although this behavior was not observed for any other GRASP so far and it seems to be unique to yeasts.

DGRASP65 is sequentially more similar to the fungi DGRASPs than DGRASP55

Eukaryotic diversity can be classified into six major divisions, or supergroups, based on phylogenomic analyses

and named Opisthokonta, Amoebozoa, Excavata, Archaeplastida, Rhizaria, and Chromalveolata [50]. The familiar model organisms of yeast and mammals are found within the Opisthokonta [50]. The Golgi apparatus is an ancient and ubiquitous organelle in eukaryotic cells [50]. Interestingly, it has been suggested before, based on a Golgi evolution phylogenetic analyses, that a GRASP65-homolog is likely to have been present in the last eukaryotic common ancestor since a GRASP65-homolog was observed in all six eukaryotic supergroups, although not in all the genomes tested [51]. We decided to analyze the sequence similarity between the DGRASPs (SPR-free sequence) in the human and the fungi, inside the Opisthokonta supergroup context, to look for correlations between the experimental data and protein sequence evolution. Our experimental data have shown that DGRASP65 shares characteristic from both DGRASP55 and fungi DGRASPs. The phylogenetic analyses support these observations (Fig. 9). The evolutionary history suggested by the phylogenetic tree supports the expected clustering between species and DGRASPs, especially the groups of DGRASP55 and DGRASP65 (Fig. 9A). Interestingly, the two outliers of the fungi DGRASPs tested are the ones used in this work, where CnDGRASP seems to be evolutionarily closer to the mammalians than the other fungi DGRASPs and the ScDGRASP is the most different DGRASP (Fig. 9A). To get information of which subgroup of mammalian DGRASPs is closer related to the fungi, we rearranged the bootstrap tree and forced a situation where the roots are in both human DGRASPs (Fig. 9B,C). This was done only to force a situation where the opposite mammalian subgroup would collapse with the fungi. When the root is on the human DGRASP55, the subgroup of DGRASP65 and the fungi DGRASPs are collapsed in a node with a

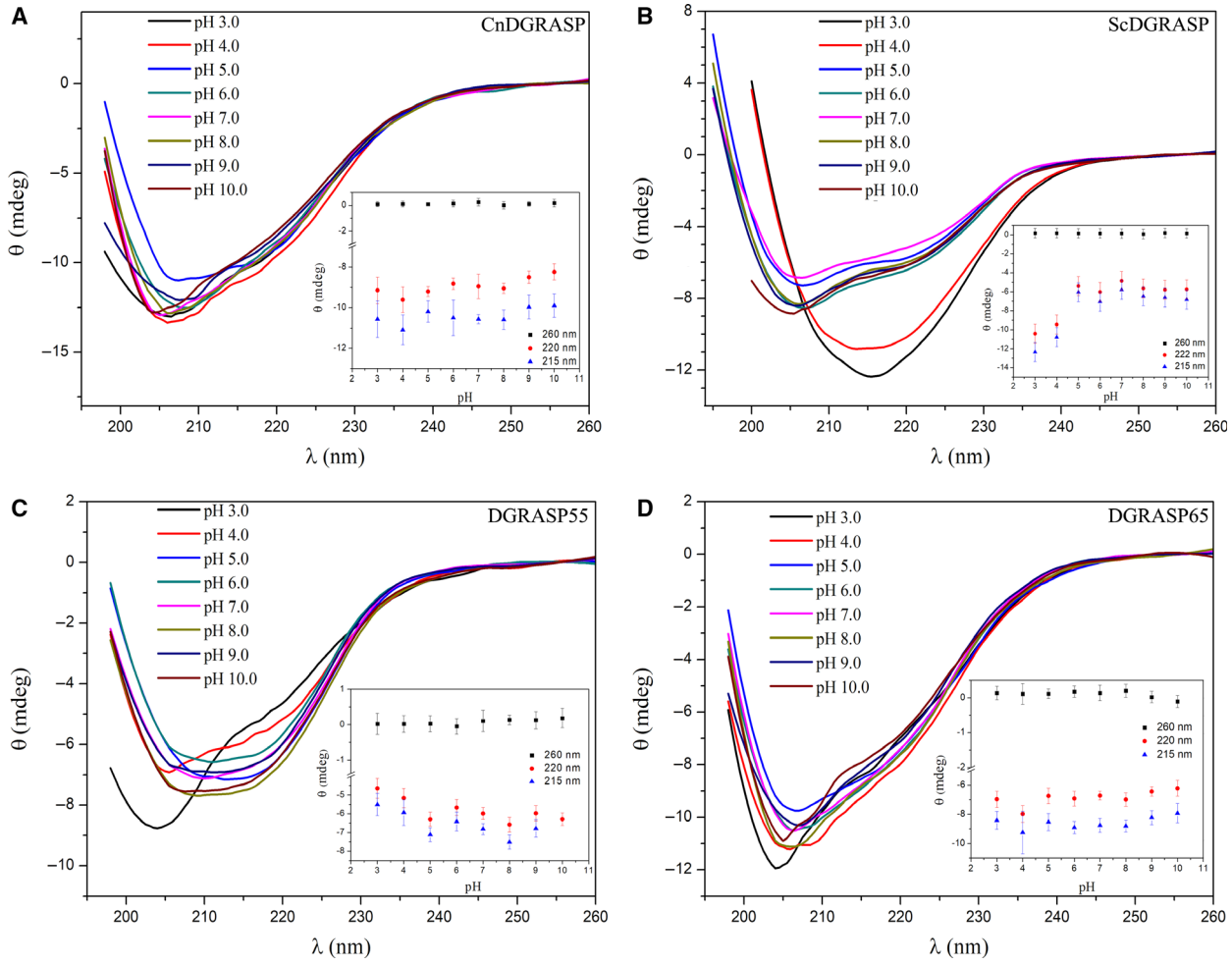

Fig. 8. Circular dichroism spectra of the GRASP domains at different pH values. The insets present the variation in the ellipticity at 260, 222, and 215 nm for each pH. Error bars represent standard deviations of triplicate measurements.

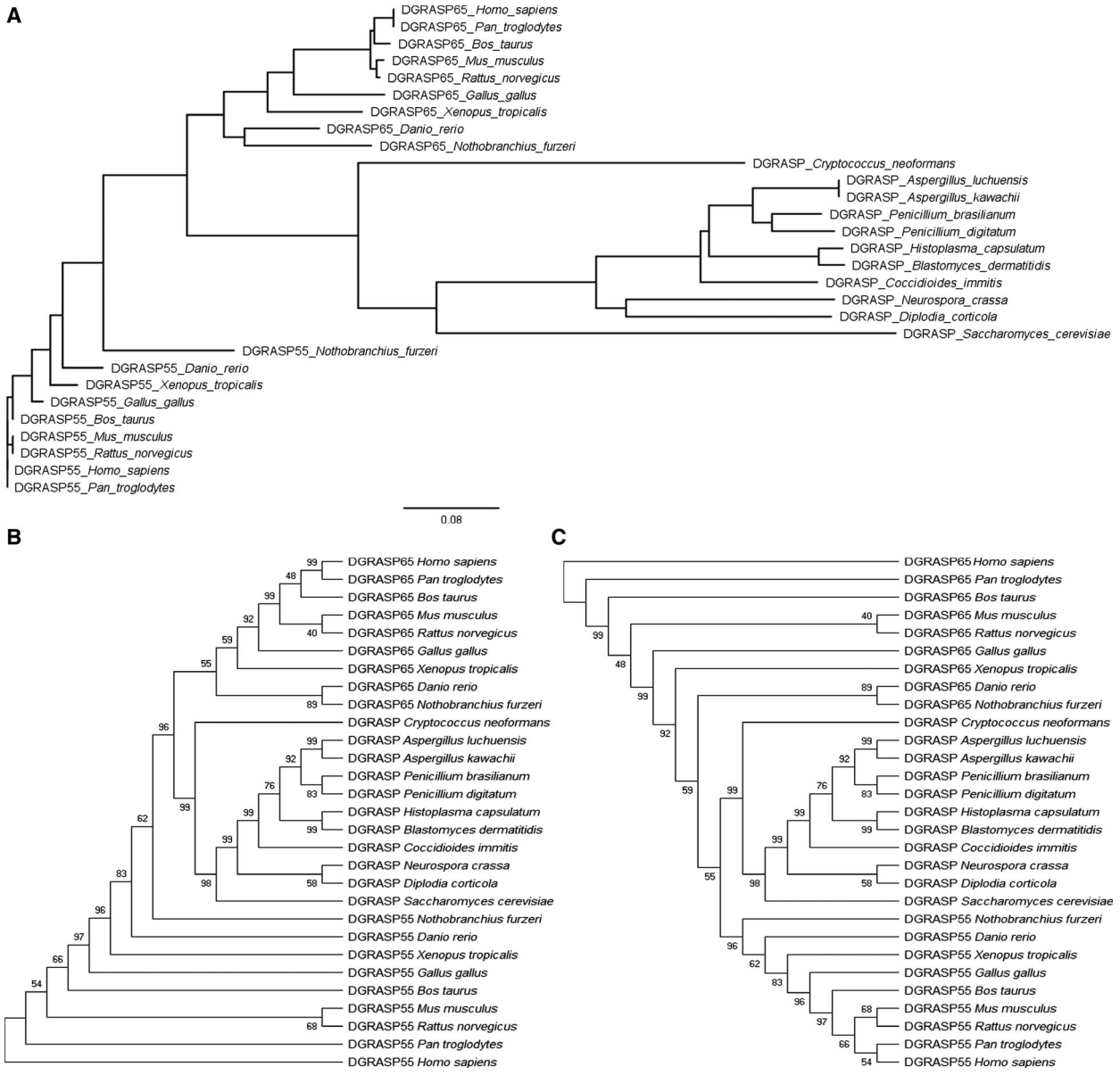

Fig. 9. The evolutionary history inferred by using the Maximum Likelihood method and JTT matrix-based model estimated using Mega X. (A) Phylogenetic tree with distance-scaled branch lengths constructed using FIGTREE v1.4.4. The MEGA X bootstrap consensus trees rooted in the (B) DGRASP55 and (C) DGRASP65 are also presented. The sequences used in this analysis are presented in the Supporting information.

bootstrap of 95, giving a high statistical significance to this arrange (Fig. 9B). However, when the root is in the human DGRASP65, the two remaining subgroups collapse in a node with a bootstrap of only 55, so it is not possible to be certain about this organization (Fig. 9C). These analyses suggest that the DGRASP65 subgroup seems to be closer than the DGRASP55 to the fungi DGRASPs in evolutionary terms. It is reasonable to speculate, from this sequence conservation, that GRASP65 might have appeared earlier in the evolution and, probably latter in mammalians; there was a GRASP65 duplication within the genome, giving rise to its paralogue GRASP55. It seems that the single fungi DGRASPs and DGRASP65 have evolved to keep a higher number of IDRs and a less packed structure, while DGRASP55 is more well-defined and well-behaved. The reasons why they are like this are still completely obscure.

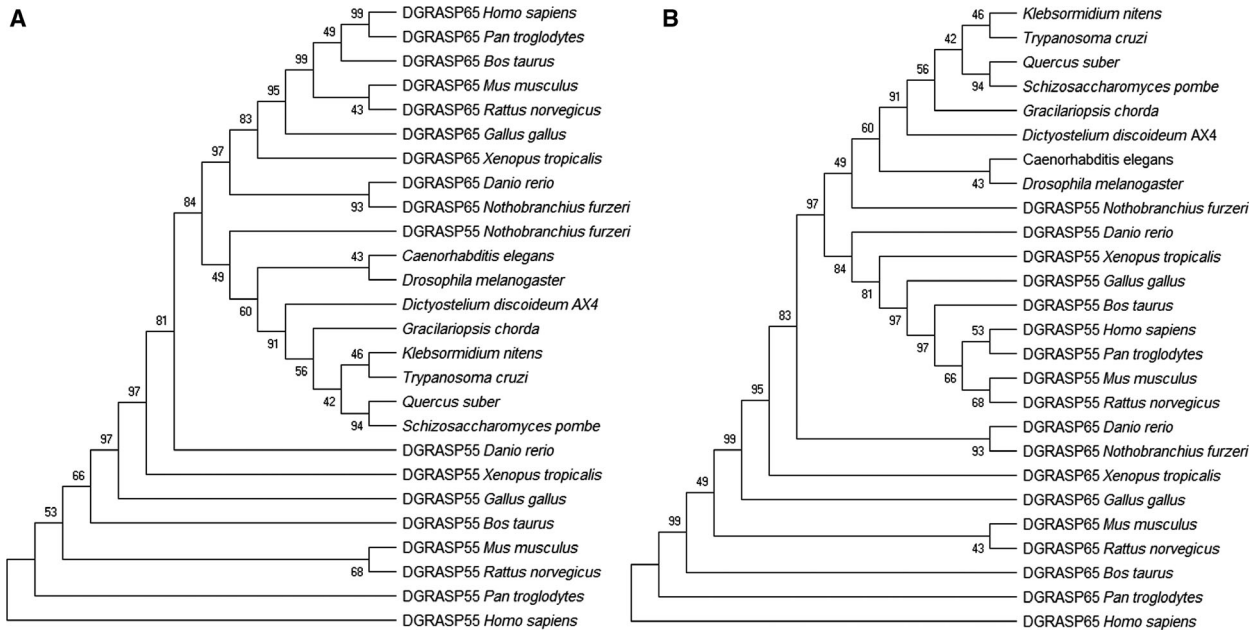

Fig. 10. The evolutionary history inferred by using the Maximum Likelihood method and JTT matrix-based model estimated using Mega X. The MEGA X bootstrap consensus trees rooted in (A) DGRASP55 and (B) DGRASP65. The sequences used in this analysis are presented in the Supporting information.

In order to check for the proximity of the GRASP55/65 family with GRASPs from other higher complexity systems compared with the fungi ones, we performed a second phylogenetic analyses including the potential GRASP orthologs from *Quercus suber (plant)* and *Gracilariopsis chorda* (red algae), and also the GRASPs from *Klebsormidium nitens* (green algae), *Caenorhabditis elegans*, *Drosophila melanogaster*, *Dictyostelium discoideum, Trypanosoma cruzi* and *Schizosaccharomyces pombe* (Fig. 10). Again, using the conserved GRASP domain only and the same methodology previously performed, we observe that the GRASP55 family has now a higher bootstrap (97) with this subgroup than the GRASP65 family (84). However, both are high bootstrap values that give only a high statistical confidence to this arrangement, which are difficult to compare in absolute terms. This is quite different from the data in Fig. 9, where the collapse between GRASP55 and the fungi gives a bootstrap value of only 55, compared to 95 between GRASP65 and the fungi, thus showing, in these two cases, significantly different values. It could be that these more evolved organisms (compared to the fungi) suffered an evolutionary pressure to have a more ordered GRASP structure (more similar to GRASP55 than the fungi), but still preserving an intermediate IDR content, thus avoiding the need of GRASP gene duplication.

Conclusions

Golgi reassembly and stacking proteins are a fundamental part of the Golgi matrix and evolved to be not only a structural factor but also a dynamic protein in other biological functions, especially UPS [9,19]. The GRASP domain is formed by two PDZ domains and this type of globule has been long described in the literature [14,31]. However, eukaryotic GRASPs are formed by PDZ domains presenting a unique fold [36]. We have previously observed unusual biophysical features of members of the GRASP family and it seems that IDRs play an important role in the structural plasticity of those proteins [30,35,39]. Nevertheless, how general is this behavior within the GRASP family and the role of the GRASP domain in these unusual biophysics observed for the full-length GRASP, are still a matter of debate. Here, we focused on the biophysical behavior in solution of four different GRASP domains: the two paralogues in humans (DGRASP55 and DGRASP65), the *S. cerevisiae* ScDGRASP (since most of the studies on UPS comes using this yeast as a model system) and the human pathogen *C. neoformans* CnDGRASP. The focus on the biophysics and not on functional studies is due to the fact that, although several interaction partners have been reported for the mammalian GRASPs [4,25,26,52], only one has appeared so far for the *S. cerevisiae*

GRASP (a predicted coiled-coil protein called BUG1) [15], and none for the *C. neoformans* GRASP. Therefore, it would have been very difficult to compare binding properties of the GRASP domains.

Our results suggest that all those DGRASPs share the same fold previously observed in the crystal structure of human DGRASP55, with CnDGRASP showing a significant higher number of disordered regions (Fig. 1). Our data also suggest that both fungi DGRASPs, which are also the solely GRASP genes found in the genome of those organisms, are enriched in IDRs and have low tertiary contacts (Figs 1, 3, 4, 5, and 7), making their transition to the unfolded state much less cooperative than those observed for general 'well-behaved' proteins. This higher IDR content makes these proteins not only more sensitive to proteolysis (Fig. 3) but also more prone to disorder-to-order transitions (Fig. 4). They also show some interesting and unique characteristics, such as CnDGRASP having a higher ANS accessibility (Fig. 6), which suggests a greater exposure of its hydrophobic core, and ScDGRASP being capable of forming fiber-like structures under some conditions (like pH, in this work, and temperature/dielectric constant variation in [39]).

On the other hand, the human DGRASP55 is the opposite of fungi DGRASPs and presents itself as a more well-structured and well-behaved protein. DGRASP55 unfolding transition takes place in a high cooperative way, does not show significant disorder-to-order transitions upon dehydration and it is very resistant to proteolytic activity. Interestingly, DGRASP55 also shows a high and impressive stability over time with no clear aggregation or unfolding after a couple of weeks at 4 °C as monitored by size-exclusion chromatography and CD spectroscopy (data not shown). It is worth noting how different DGRASP55 and the fungi DGRASPs are in biophysical means, even though they seem to share a similar fold. However, DGRASP65 seems to be placed in an intermediate state between DGRASP55 and the fungi DGRASPs and present higher content of IDRs compared to DGRASP55, but still less than the fungi DGRASPs, which leads to an intermediate proteolysis sensitivity and no effects upon dehydration. Its unfolding also presents a very low cooperative transition, similar to what is obtained for the CnDGRASP. NMR was used to give higher resolution information on these IDRS and the data thus obtained agree with all the aforementioned results. The alignment of the primary sequences shows that DGRASP65 seems to be closer to the fungi DGRASPs in that respect.

It is important to emphasize that the differences between the physiological temperatures of humans and the fungi would not interfere in the analyses performed in this work. The organisms evolved to couple the structural stability with the necessary flexibility for that particular temperature where they live. In this particular situation, a way of promoting the folding, thus increasing the protein stability, is to decrease the entropy variation in the unfolded state [53]. For example, hyperthermophile proteins are shorter in flexible regions and by doing this they decrease their flexibility, increasing the total structure stability [54]. This happens because of the inherent flexibility of loops and intrinsically disordered regions (IDRs), so they are considered as potential initiation points for thermal denaturation. As could be expected, when the temperature is decreased, these proteins are completely rigid [54]. In this context and considering the optimal physiological temperature of humans (37 °C), *C. neoformans* (34 °C [55]) and *S. cerevisiae* (30–35 °C [56]), we could expect that the high flexibility and low stability we observed for human DGRASP55 and DGRASP65 would probably be even more accentuated at increased temperatures. Besides, IDRs were not disordered because of temperature (or any other environment-related parameter), but as an intrinsic consequence of its amino acid content [57]. IDRs, just like fully intrinsically disordered proteins, have unusual biophysics but not the same as the unfolded structures or loops [33,57]. Therefore, DGRASP55 or DGRASP65 would not necessarily be more/less disordered in higher/lower temperatures.

Based in all the data presented in this manuscript, we hypothesize that the last common ancestor of fungi and humans, probably where the whole Opisthokonta supergroup diverged from the others, presented a GRASP homolog that shared the characteristics of ScGRASP, CnGRASP, and GRASP65. Later in evolution, a gene duplication might led to the paralogue GRASP55 appearance and this protein evolved to be a more well-structured protein for some still unknown reason. Probably this was the same evolutionary pressure that acted on the *Plasmodium falciparum* gene to evolve for two GRASP isoforms coming from an alternate splicing [17], one similar to GRASP55/65 and the other to the fungi ones. This higher biophysical similarity between DGRASP65 and the fungi DGRASPs would be reasonable if one thinks within the Golgi structure context, since most of the fungi have unstacked (or only partially stacked) Golgi complex and, in the reference of an unstacked, free cisternae, facing the ER, this would be more similar to the *cis*-Golgi face in mammalian cells. Since GRASP65 is present mainly in the *cis*-Golgi structure, while GRASP55 populates the *medial* and *trans*-faces, it would make

sense to observe more similarity in the biophysical properties of GRASP65 and the fungi ones.

Materials and methods

Protein expression and purification

Cryptococcus neoformans GRASP domain (CnDGRASP) and *S. cerevisiae* GRASP domain (ScDGRASP) were expressed and purified as discussed elsewhere [30,39]. Human GRASP55 and GRASP65 genes were synthesized with a codon-optimization for *E. coli* expression and the GRASP domain of GRASP55 (1-208) and of GRASP65 (1-211) were amplified by PCR and subcloned into the pWALDO-d vector using the Nde1 and BamH1 sites and further transformed into Rosetta (DE3) cells. Liquid inoculum of LB medium was used for cell growth at 37 °C until OD_{600} nm of 1.0 was obtained. Protein expression was induced by adding Isopropyl-β-D-thiogalactoside at a final concentration of 0.5 mM for 18 h at 20 °C and 220 r.p.m. Cells were sedimented by centrifugation (7000 ***g*** per 5 min at 4 °C) and resuspended in a solution of 20 mM Tris-HCl, 150 mM NaCl, 10 mM 2-Mercaptoethanol, 0.5% Triton X-100 and 250 μM PMSF, pH 8.0. Cells were disrupted by sonication and clarified by centrifugation (18 000 ***g*** per 20 min at 4 °C). The soluble fraction was loaded into a Ni-nitrilotriacetic acid column, and the bound protein was washed with 20 mM Tris-HCl, 150 mM NaCl, 10 mM 2-Mercaptoethanol, pH 8.0 (buffer A), buffer A + 20 mM imidazole, buffer A + 50 mM imidazole and eluted with buffer A + 500 mM imidazole. Two milligrams of purified TEV was added for each liter of expressed GRASP55 or GRASP65 GRASP domain (DGRASP55 and DGRASP65, respectively, from now on) and the final solution (around 15 mL) was dialyzed against 4 L of 20 mM Tris-HCl pH 8.0, 50 mM NaCl and 7 mM 2-Mercaptoethanol, overnight at 4 °C. The solution was then reloaded into a Ni-nitrilotriacetic acid column and the super flow was collected, concentrated, and applied in a Mono Q 5/50 GL (GE Healthcare Life Sciences, Chicago, IL, USA) coupled with an *Äkta purifier* system (GE Healthcare). The protein solution was submitted to a linear gradient of NaCl from 50 to 350 mM (25 mM Tris-HCl pH 8.0, 10 mM 2-Mercaptoethanol). The fractions corresponding to pure DGRASP55/65 were then concentrated and applied into a Superdex200 10/300 GL gel filtration column (GE Healthcare Life Sciences) equilibrated in a 25 mM Tris-HCl pH 8.0, 150 mM NaCl, 7 mM 2-Mercaptoethanol. For protein concentration, an Amicon Ultra-15 Centrifugal Filter with a NMWL of 10 kDa (Merck Millipore, Burlington, MA, USA) was used. Protein concentration was measured using the extinction coefficient at 280 nm calculated using protparam webserver [58] considering the non-native amino acids present at the C terminus after TEV cleavage. For DGRASP55, the $\varepsilon_{280\ nm}$ = 28 420 $M^{-1}{\cdot}cm^{-1}$ and Abs 0.1% (=1 $mg{\cdot}mL^{-1}$) 1.199, while for DGRASP65 is $\varepsilon_{280\ nm}$ = 28 420 $M^{-1}{\cdot}cm^{-1}$; Abs 0.1% (=1 $mg{\cdot}mL^{-1}$) 1.182 were used. For CnDGRASP and ScDGRASP, the parameters were as presented elsewhere [30,39].

Circular dichroism

Conventional far-UV CD experiments were performed in a Jasco J-815 CD Spectrometer (JASCO Corporation, Easton, MD, USA) equipped with a Peltier temperature control and using a quartz cell with a 1-mm path length. The spectra were recorded from 260 to 198 nm, with a scanning speed of 100 $nm{\cdot}min^{-1}$, spectral bandwidth of 1 nm, response time of 0.5 s and taking individual measurements prior to the average in order to check protein instability after the final spectra. All the protein stock solutions were at a minimum concentration where the dilution in a 20 mM sodium phosphate pH 8.0 (or any desired buffer) was at least 20-fold. Urea denaturation was carried out in a 0.8 M urea steps with an overnight incubation at 4 °C and a 1-h incubation period at 25 °C prior to the measurements. Experiments with pH variation were performed with the same criteria of dilution in a 20 mM glycine HCl (pH 3.0), 20 mM sodium acetate/acetic acid (pH 4.0), 20 mM sodium phosphate (pH 5.0–8.0), or 20 mM glycine NaOH (pH 9.0 and 10.0) with an incubation time of 10 min at 25 °C. All the experiments were performed at 25 °C. CD spectra reconstruction was performed using PDB2CD [40].

Synchrotron Radiation Circular Dichroism spectroscopy

Synchrotron Radiation Circular Dichroism spectroscopy was employed to access the lower wavelength UV region with an improved signal-to-noise ratio and to characterize conformational changes (significant or subtle) with higher accuracy than the conventional method. The SRCD spectra of the proteins in aqueous solution were collected at the AU-CD beamline at the Institute for Storage Ring facilities (ASTRID2 synchrotron), University of Aarhus, Denmark. Measurements were performed taking three successive scans over the wavelength range from 280 to 180 nm, using 1-nm interval and 2-s dwell time, at 25 °C, and a 0.01027-cm path length cylindrical Suprasil quartz cell (Hellma Ltd., Southend-on-Sea, UK). Additionally, aliquots (0.7 nmol) of each protein were deposited on the surface of a quartz-glass plate to form a partially dried film of the proteins, promoting the evaporation of the solution under moderate vacuum. The SRCD spectrum of the dehydrated film was collected over the range 280–160 nm, with a 1-nm interval and 2-s dwell time, at 25 °C, taking four different rotations of the plate (0, 90, 180, and 270 degrees) in order to avoid linear dichroism effect. CDTOOLX [59] software was used for all SRCD data processing, which consisted of performing the average of the three individual scans collected from each sample, baseline subtraction (spectra taken of each

corresponding buffer with all additives, except for the protein), zeroing at the region at 263–270 nm, smoothing with a Savitky–Golay filter, calibration against a spectrum of a camphoursulphonic acid standard taken at the beginning of the data collection, and final data expressed in delta epsilon units. CD spectra deconvolution was performed using the webserver DICHROWEB [60,61] and selecting the reference set SP175 optimized for 190–240 nm.

Fluorescence spectroscopy

Steady-state fluorescence was monitored using a Hitachi F-7000 spectrofluorometer equipped with a 150 W xenon arc lamp. The excitation and emission monochromators were set at a 5-nm slit width in all tryptophan experiments and 5-nm excitation with 10 nm emission for the ANS experiments. The protein concentrations were 15 μM. For tryptophan fluorescence experiments, the selective tryptophan excitation wavelength was set at 295 nm and the emission spectra were measured from 310 up to 450 nm. For the 1-anilino-8-naphthalenesulfonic acid (ANS—250 μM) fluorescence experiments, the excitation wavelength was set at 360 nm and the emission spectra were measured from 400 up to 650 nm. Fluorescence quenching using the water-soluble acrylamide as a quencher was performed in a serial dilution from an 8 M acrylamide stock solution with 5 min thermal equilibration. All the experiments were performed at 25 °C.

Bioinformatic analyses

Multiple sequence alignment using seeded guide trees and Hidden Markov Model profile-profile techniques were performed using Clustal Omega [62]. The evolutionary history was inferred by using the Maximum Likelihood method and JTT matrix-based model [63]. The bootstrap consensus tree inferred from 10 000 replicates is taken to represent the evolutionary history of the taxa analyzed. Branches corresponding to partitions reproduced in less than 50% bootstrap replicates are collapsed. The percentages of replicate trees in which the associated taxa clustered together in the bootstrap test (10 000 replicates) are shown next to the branches. Initial tree(s) for the heuristic search were obtained automatically by applying neighbor-joining and BioNJ algorithms to a matrix of pairwise distances estimated using a JTT model, and then selecting the topology with superior log likelihood value. Evolutionary analyses were conducted in MEGA X [64]. Protein theoretical pI was estimated using Protparam webserver [58]. Protein structure homology modeling was performed with Swiss-MODEL [65] and the sequences used are presented in the supporting information.

Limited proteolysis

Proteolysis sensitivity was assessed using trypsin from bovine pancreas (Sigma-Aldrich, St. Louis, MO, USA) in a molar ratio (protein/trypsin) of 100/1 at 25 °C. Ovalbumin (GE Life Science) was used as a model of well-structured proteins for direct comparison. Adding SDS/PAGE buffer and heating at 95 °C for 10 min quenched the reactions. All reactions were checked by Coomassie stained 15% SDS/PAGE.

Nuclear magnetic resonance

The NMR spectra of ^{15}N-DGRASPs (concentration around 100 μM) were recorded at 25 °C in an NMR spectrometer equipped with cryogenically cooled z-gradient probe operating at ^{1}H frequency of 600 MHz (Bruker BioSpin GmbH, Rheinstetten, Germany) and using a Shigemi 5-mm symmetrical NMR microtube assembly (Sigma-Aldrich). Protein expression in minimum media supplemented with $^{15}NH_4Cl$ was performed using a protocol presented elsewhere [66]. Cell induction and protein purification were performed using the same protocol described earlier for the unlabeled samples, except for a change in the solution used in the gel filtration step, where now a 25 mM HEPES/NaOH, 100 mM NaCl, 7 mM 2-Mercaptoethanol, pH 7.0 was used. A final volume of 5% D_2O was added to each sample. The data were processed and analyzed using TopSpin 3.5.

Acknowledgements

The authors thank the Brazilian agencies Conselho Nacional de Desenvolvimento Científico e Tecnológico (CNPq) and Fundação de Amparo à Pesquisa do Estado de São Paulo (FAPESP) for the financial support through Grants No. 2015/50366-7, 2012/20367-3, and 308380/2013-4. LFSM and NAF acknowledge FAPESP for the postdoctoral (Grant No. 2017/24669-8) and PhD fellowship grants (Grant No. 2016/23863-2), respectively. JLSL is grateful for the financial support 303513/2016-0 from the CNPq-Brazil. The authors also thank the Multiuser Center for Biomolecular Innovation (EMU-Fapesp Grant No. 2009/53989-4) for the access to the NMR machine, and to ASTRID2 synchrotron at University of Aarhus, Denmark, for the access to the AU-CD beamline (beamtime grants to JLSL).

Conflict of interest

The authors declare no conflict of interest.

Author contributions

LFSM performed most of the experimental procedures and the analyses. NAF, MCLCF, CGO, JLSL, and FAM were involved in part of the experimental procedures and/or analyses. AJCF conceived and

coordinated the project. All authors contributed to the writing and reviewing of the results. All authors also approved the final version of the manuscript.

References

1 Marsh BJ & Howell KE (2002) The mammalian Golgi–complex debates. *Nat Rev Mol Cell Biol* **3**, 789–95.
2 Mellman I & Simons K (1992) The Golgi complex: in vitro veritas? *Cell* **68**, 829–40.
3 Xiang Y, Zhang X, Nix DB, Katoh T, Aoki K, Tiemeyer M & Wang Y (2013) Regulation of protein glycosylation and sorting by the Golgi matrix proteins GRASP55/65. *Nat Commun* **4**, 1659.
4 Barr FA, Preisinger C, Kopajtich R & Körner R (2001) Golgi matrix proteins interact with p24 cargo receptors and aid their efficient retention in the Golgi apparatus. *J Cell Biol* **155**, 885–91.
5 Banfield DK (2011) Mechanisms of protein retention in the Golgi. *Cold Spring Harb Perspect Biol* **3**, a005264.
6 Barr FA, Puype M, Vandekerckhove J & Warren G (1997) GRASP65, a protein involved in the stacking of Golgi cisternae. *Cell* **91**, 253–262.
7 Shorter J, Watson R, Giannakou ME, Clarke M, Warren G & Barr FA (1999) GRASP55, a second mammalian GRASP protein involved in the stacking of Golgi cisternae in a cell-free system. *EMBO J* **18**, 4949–60.
8 Xiang Y & Wang Y (2010) GRASP55 and GRASP65 play complementary and essential roles in Golgi cisternal stacking. *J Cell Biol* **188**, 237–51.
9 Rabouille C & Linstedt AD (2016) GRASP: A multitasking tether. *Front Cell Dev Biol* **4**, 1.
10 Bekier ME 2nd, Wang L, Li J, Huang H, Tang D, Zhang X & Wang Y (2017) Knockout of the Golgi stacking proteins GRASP55 and GRASP65 impairs Golgi structure and function. *Mol Biol Cell* **28**, 2833–2842.
11 Bachert C & Linstedt AD (2010) Dual anchoring of the GRASP membrane tether promotes trans pairing. *J Biol Chem* **285**, 16294–301.
12 Manca S, Frisbie CP, LaGrange CA, Casey CA, Riethoven JM & Petrosyan A (2019) The role of alcohol-induced Golgi fragmentation for androgen receptor signaling in prostate cancer. *Mol Cancer Res* **17**, 225–37.
13 Zhang N, Prasad S, Huyghues Despointes CE, Young J & Kima PE (2018) Leishmania parasitophorous vacuole membranes display phosphoinositides that create conditions for continuous Akt activation and a target for miltefosine in Leishmania infections. *Cell Microbiol* **20**, e12889.
14 Vinke FP, Grieve AG & Rabouille C (2011) The multiple facets of the Golgi reassembly stacking proteins. *Biochem J* **433**, 423–33.
15 Behnia R, Barr FA, Flanagan JJ, Barlowe C & Munro S (2007) The yeast orthologue of GRASP65 forms a complex with a coiled-coil protein that contributes to ER to Golgi traffic. *J Cell Biol* **176**, 255–61.
16 Kmetzsch L, Joffe LS, Staats CC, de Oliveira DL, Fonseca FL, Cordero RJ, Casadevall A, Nimrichter L, Schrank A, Vainstein MH *et al.* (2011) Role for Golgi reassembly and stacking protein (GRASP) in polysaccharide secretion and fungal virulence. *Mol Microbiol* **81**, 206–18.
17 Struck NS, Herrmann S, Langer C, Krueger A, Foth BJ, Engelberg K, Cabrera AL, Haase S, Treeck M, Marti M *et al.* (2008) Plasmodium falciparum possesses two GRASP proteins that are differentially targeted to the Golgi complex via a higher- and lower-eukaryote-like mechanism. *J Cell Sci* **121** (Pt 13), 2123–9.
18 Giuliani F, Grieve A & Rabouille C (2011) Unconventional secretion: a stress on GRASP. *Curr Opin Cell Biol* **23**, 498–504.
19 Rabouille C (2017) Pathways of unconventional protein secretion. *Trends Cell Biol* **27**, 230–240.
20 Zhang X & Wang Y (2018) The Golgi stacking protein GORASP2/GRASP55 serves as an energy sensor to promote autophagosome maturation under glucose starvation. *Autophagy* **14**, 1649–1651.
21 Zhang X, Wang L, Lak B, Li J, Jokitalo E & Wang Y (2018) GRASP55 senses glucose deprivation through O-GlcNAcylation to promote autophagosome-lysosome fusion. *Dev Cell* **45**, 245–261.e6.
22 Gee HY, Noh SH, Tang BL, Kim KH & Lee MG (2011) Rescue of ΔF508-CFTR trafficking via a GRASP-dependent unconventional secretion pathway. *Cell* **146**, 746–60.
23 Nüchel J, Ghatak S, Zuk AV, Illerhaus A, Mörgelin M, Schönborn K, Blumbach K, Wickström SA, Krieg T, Sengle G *et al.* (2018) TGFB1 is secreted through an unconventional pathway dependent on the autophagic machinery and cytoskeletal regulators. *Autophagy* **14**, 465–486.
24 Kuo A, Zhong C, Lane WS & Derynck R (2000) Transmembrane transforming growth factor-alpha tethers to the PDZ domain-containing, Golgi membrane-associated protein p59/GRASP55. *EMBO J* **19**, 6427–39.
25 Dementieva IS, Tereshko V, McCrossan ZA, Solomaha E, Araki D, Xu C, Grigorieff N & Goldstein SA (2009) Pentameric assembly of potassium channel tetramerization domain-containing protein 5. *J Mol Biol* **387**, 175–91.
26 Cartier-Michaud A, Bailly AL, Betzi S, Shi X, Lissitzky JC, Zarubica A, Sergé A, Roche P, Lugari A, Hamon V *et al.* (2017) Genetic, structural, and chemical insights into the dual function of GRASP55 in germ cell Golgi remodeling and JAM-C polarized localization during spermatogenesis. *PLoS Genet* **13**, e1006803.
27 Cruz-Garcia D, Curwin AJ, Popoff JF, Bruns C, Duran JM & Malhotra V (2014) Remodeling of secretory

compartments creates CUPS during nutrient starvation. *J Cell Biol* **207**, 695–703.
28 Bruns C, McCaffery JM, Curwin AJ, Duran JM & Malhotra V (2011) Biogenesis of a novel compartment for autophagosome-mediated unconventional protein secretion. *J Cell Biol* **195**, 979–92.
29 Zahoor M & Farhan H (2018) Crosstalk of autophagy and the secretory pathway and its role in diseases. *Int Rev Cell Mol Biol* **337**, 153–184.
30 Mendes LF, Garcia AF, Kumagai PS, de Morais FR, Melo FA, Kmetzsch L, Vainstein MH, Rodrigues ML & Costa-Filho AJ (2016) New structural insights into Golgi Reassembly and Stacking Protein (GRASP) in solution. *Sci Rep* **6**, 29976.
31 Wang Y, Satoh A & Warren G (2005) Mapping the functional domains of the Golgi stacking factor GRASP65. *J Biol Chem* **280**, 4921–8.
32 Lane JD, Lucocq J, Pryde J, Barr FA, Woodman PG, Allan VJ & Lowe M (2002) Caspase-mediated cleavage of the stacking protein GRASP65 is required for Golgi fragmentation during apoptosis. *J Cell Biol* **156**, 495–509.
33 Uversky VN (2013) Unusual biophysics of intrinsically disordered proteins. *Biochim Biophys Acta* **1834**, 932–51.
34 Sigalov AB (2016) Structural biology of intrinsically disordered proteins: Revisiting unsolved mysteries. *Biochimie* **125**, 112–8.
35 Mendes LFS, Basso LGM, Kumagai PS, Fonseca-Maldonado R & Costa-Filho AJ (2018) Disorder-to-order transitions in the molten globule-like Golgi Reassembly and Stacking Protein. *Biochim Biophys Acta Gen Subj* **1862**, 855–865.
36 Truschel ST, Sengupta D, Foote A, Heroux A, Macbeth MR & Linstedt AD (2011) Structure of the membrane-tethering GRASP domain reveals a unique PDZ ligand interaction that mediates Golgi biogenesis. *J Biol Chem* **286**, 20125–9.
37 Feng Y, Yu W, Li X, Lin S, Zhou Y, Hu J & Liu X (2013) Structural insight into Golgi membrane stacking by GRASP65 and GRASP55 proteins. *J Biol Chem* **288**, 28418–27.
38 Lee HJ & Zheng JJ (2010) PDZ domains and their binding partners: structure, specificity, and modification. *Cell Commun Signal* **8**, 8.
39 Fontana NA, Fonseca-Maldonado R, Mendes LFS, Meleiro LP & Costa-Filho AJ (2018) The yeast GRASP Grh1 displays a high polypeptide backbone mobility along with an amyloidogenic behavior. *Sci Rep* **8**, 15690.
40 Mavridis L & Janes RW (2017) PDB2CD: a web-based application for the generation of circular dichroism spectra from protein atomic coordinates. *Bioinformatics* **33** (1), 56–63.
41 Tompa P (2009) Structure and function of intrinsically disordered proteins. CRC Press, Boca Raton, FL.
42 Yoneda JS, Miles AJ, Araujo AP & Wallace BA (2017) Differential dehydration effects on globular proteins and intrinsically disordered proteins during film formation. *Protein Sci* **26**, 718–726.
43 Kelly SM, Jess TJ & Price NC (2005) How to study proteins by circular dichroism. *Biochim Biophys Acta* **1751**, 119–139.
44 Malhotra P & Udgaonkar JB (2016 Nov) How cooperative are protein folding and unfolding transitions? *Protein Sci* **25**, 1924–1941.
45 DeForte S & Uversky VN (2016) Order, disorder, and everything in between. *Molecules* **21**, 1090.
46 Feng Y, Yu W, Li X, Lin S, Zhou Y, Hu J & Liu X (2011) Structural insight into Golgi membrane stacking by GRASP65 and GRASP55 proteins. *J Biol Chem* **288**, 28418–27.
47 Hu F, Shi X, Li B, Huang X, Morelli X & Shi N (2015) Structural basis for the interaction between the Golgi reassembly-stacking protein GRASP65 and the Golgi matrix protein GM130. *J Biol Chem* **290**, 26373–82.
48 Carugo O (2018) How large B-factors can be in protein crystal structures. *BMC Bioinformatics* **19**, 61.
49 Uversky VN (2009) Intrinsically disordered proteins and their environment: effects of strong denaturants, temperature, pH, counter ions, membranes, binding partners, osmolytes, and macromolecular crowding. *Protein J* **28**, 305–25.
50 Burki F (2014) The eukaryotic tree of life from a global phylogenomic perspective. *Cold Spring Harb Perspect Biol* **6**, a016147.
51 Barlow LD, Nývltová E, Aguilar M, Tachezy J & Dacks JB (2018) A sophisticated, differentiated Golgi in the ancestor of eukaryotes. *BMC Biol* **16**, 27.
52 Short B, Preisinger C, Körner R, Kopajtich R, Byron O & Barr FA (2001) A GRASP55-rab2 effector complex linking Golgi structure to membrane traffic. *J Cell Biol* **155**, 877–83.
53 Shakhnovich E (2006) Protein folding thermodynamics and dynamics: where physics, chemistry, and biology meet. *Chem Rev* **106**, 1559–88.
54 Reed CJ, Lewis H, Trejo E, Winston V & Evilia C (2013) Protein adaptations in archaeal extremophiles. *Archaea* **2013**, 373275.
55 Madeira-Lopes A & Van Uden N (1982) The temperature profile of *Cryptococcus neoformans*. *Sabouraudia* **20**, 331–4.
56 Xu X, Lambrecht AD & Xiao W (2014) Yeast survival and growth assays. *Methods Mol Biol* **1163**, 183–91.
57 Uversky VN, Gillespie JR & Fink AL (2000) Why are "natively unfolded" proteins unstructured under physiologic conditions? *Proteins*. **41**, 415–27.
58 Wilkins MR, Gasteiger E, Bairoch A, Sanchez JC, Williams KL, Appel RD & Hochstrasser DF (1999) Protein identification and analysis tools in the ExPASy server. *Methods Mol Biol* **112**, 531–52.

59 Miles AJ & Wallace BA (2018) CDtoolX, a downloadable software package for processing and analyses of circular dichroism spectroscopic data. *Protein Sci* **27**, 1717–1722.
60 Whitmore L & Wallace BA (2008) Protein secondary structure analyses from circular dichroism spectroscopy: methods and reference databases. *Biopolymers* **89**, 392–400.
61 Whitmore L & Wallace BA (2004) DICHROWEB, an online server for protein secondary structure analyses from circular dichroism spectroscopic data. *Nucleic Acids Res* **32**(Web Server issue), W668–73.
62 Sievers F, Wilm A, Dineen D, Gibson TJ, Karplus K, Li W, Lopez R, McWilliam H, Remmert M, Söding J *et al*. (2011) Fast, scalable generation of high-quality protein multiple sequence alignments using Clustal Omega. *Mol Syst Biol* **7**, 539.
63 Jones DT, Taylor WR & Thornton JM (1992) The rapid generation of mutation data matrices from protein sequences. *Comput Appl Biosci* **8**, 275–82.
64 Kumar S, Stecher G, Li M, Knyaz C & Tamura K (2018) MEGA X: Molecular evolutionary genetics analysis across computing platforms. *Mol Biol Evol* **35**, 1547–1549.
65 Waterhouse A, Bertoni M, Bienert S, Studer G, Tauriello G, Gumienny R, Heer FT, de Beer TAP, Rempfer C, Bordoli Lepore R *et al*. (2018) SWISS-MODEL: homology modelling of protein structures and complexes. *Nucleic Acids Res* **46**, W296–W303.
66 Protocol from the NMR Structural Biology Facility from UConn Health webserver https://health.uconn.edu/structural-biology/wp-content/uploads/sites/177/2017/10/nmr_sample_preparation.pdf (accessed in 2018).

Supporting information

Additional supporting information may be found online in the Supporting Information section at the end of the article.

Appendix S1 List of DGRASPs used in this work presented in a fasta format.